Journal of Bioscience and Bioengineering
VOL. 127 No. 4, 520–527, 2019

www.elsevier.com/locate/jbiosc

High-sensitive liquid chromatography-tandem mass spectrometry-based chiral metabolic profiling focusing on amino acids and related metabolites

Yosuke Nakano, Moyu Taniguchi, and Eiichiro Fukusaki*

Department of Biotechnology, Graduate School of Engineering, Osaka University, 2-1 Yamadaoka, Suita, Osaka 565-0871, Japan

Received 24 June 2018; accepted 4 October 2018
Available online 15 December 2018

Metabolomics has been an evolving science with a wide range of applications in various fields. However, previous studies have rarely focused on metabolite chirality. In this study, to achieve metabolic profiling of chiral amino acids and related metabolites, we developed a high-throughput method using liquid chromatography-tandem mass spectrometry (LC-MS/MS). The combination of two types of chiral columns (with binaphthyl-based crown ether and cinchona alkaloid-derived zwitterionic stationary phases) enabled the analysis of 115 chiral and non-chiral metabolites. By finely optimizing MS/MS parameters, the method allowed the highly sensitive (0.001–50 nmol/mL) and wide dynamic range detection of targeted analytes in a standard solution without derivatization. We applied the method to food samples (cheese), and successfully quantified trace levels of metabolites such as D-amino acids in samples. Additionally, we performed principal component analysis on the metabolome data and obtained unique profiles that reflected metabolite chirality. These results demonstrated the applicability and feasibility of the LC-MS/MS method as an effective tool for wide-targeted chiral metabolome analysis.

[**Key words:** D-Amino acid; Chiral metabolomics; Enantioseparation; Liquid chromatography-tandem mass spectrometry; Cheese]

To realize authentic metabolomics, namely to perform comprehensive analysis of metabolites, it is necessary to analyze metabolite chirality. Many previous studies have addressed the importance of chiral analysis because some enantiomers possess different toxicities and biological activities (1–3). Enantioseparation of amino acids has recently attracted much attention in various research fields including medical, clinical, and food industries. In α-amino acids, both the carboxylic acid group and amino group are bonded to the same carbon center and there are many variations of the side chains. Due to this configuration, the structure can form enantiomers. Generally, to distinguish these structures, they are commonly referred to as L- or D-amino acids. L-Amino acids are the predominant building blocks of proteins while D-amino acids cannot be incorporated into proteins via ribosomal synthesis (4) and it was believed for a long time that D-amino acids are not present in mammals (5). However, recent technological advances in separation techniques have permitted studies on D-amino acids. D-Serine exists in mammals, especially in the brain, and activates the *N*-methyl-D-aspartic acid (NMDA) receptor as its co-agonist (6,7) leading to mental disorders such as schizophrenia (8–10). D-Aspartic acid is present in invertebrate and vertebrate neuroendocrine tissues (11) and is involved in regulating hormone secretion (12–14). Further, some D-amino acids are associated with kidney function and thus are potential biomarkers of kidney diseases (15).

A number of reports demonstrated the enantioseparation of chiral metabolites, including amino acids, by chromatographic technologies such as thin layer chromatography (TLC) (16,17), gas chromatography (GC) (18,19), and high-performance liquid chromatography (HPLC) (20–22). Recently, we developed analytical methods for the simultaneous analysis of eighteen chiral proteinogenic amino acids using a combination of a chiral crown ether column and liquid chromatography-time of flight mass spectrometry (LC-TOFMS) (23) or liquid chromatography-tandem mass spectrometry (LC-MS/MS) (24). These methods enabled the baseline enantioseparation of amino acids while maintaining excellent peak resolution. Moreover, these methods require no derivatization steps and thus can avoid undesirable issues that may occur during derivatization. Most recently, we expanded the coverage of targeted metabolites and consequently succeeded in the enantioseparation of chiral non-proteinogenic amino acids and amines using LC-TOFMS (25). This method is anticipated to aid in chiral metabolomics; but there are some limitations on the expansion of targeted metabolites and the improvement of sensitivity using TOFMS.

In this study, we aimed to develop an effective method for the simultaneous analysis of chiral non-proteinogenic amino acids, amines, and nucleic acid metabolites in addition to chiral proteinogenic amino acids. First, we fine-tuned various MS/MS parameters to achieve the highly sensitive detection of targeted metabolites without derivatization. Compared to TOFMS, MS/MS is widely recognized as a powerful analytical tool for providing quantitative data. Multiple reaction monitoring (MRM) mode in MS/MS employs two stages of mass filtering that can remove impurity ions, which enables highly sensitive and selective detection of trace target compounds. Next, we verified the separation

* Corresponding author. Tel./fax: +81 6879 7424.
E-mail address: fukusaki@bio.eng.osaka-u.ac.jp (E. Fukusaki).

1389-1723/$ – see front matter
https://doi.org/10.1016/j.jbiosc.2018.10.003

conditions of the method in accordance with our previous reports. We also examined the enantioseparation of secondary amines including proline, which were impossible to separate enantiomerically due to their insufficient interaction with the default separation column. After evaluating the method for the validation, we finally applied the method to the quantitative analysis of targeted metabolites contained in food (cheese) and confirmed the feasibility of the novel method.

MATERIALS AND METHODS

Reagents Standards (chiral proteinogenic amino acids, non-proteinogenic amino acids, and amines) and internal standards (DL-alanine-2,3,3,3-d_4) were purchased from Tokyo Chemical Industry Co., Ltd. (Tokyo, Japan), Sigma–Aldrich Japan K.K. (Tokyo, Japan), Fujifilm Wako Pure Chemical Corporation, (Osaka, Japan), Kishida Chemical Co., Ltd. (Osaka, Japan), Nacalai Tesque, Inc. (Kyoto, Japan), Acros Organics (Geel, Belgium), or Santa Cruz Biotechnology (Dallas, TX, USA). For preparation of the mobile phase and sample pretreatment, ultrapure water for LC/MS (water), 0.1 mol/L hydrochloric acid for volumetric analysis (HCl), 1 mol/L ammonium formate solution (AF), and formic acid (FA) were obtained from Wako. Methanol Plus for LC/MS (MeOH), acetonitrile Plus for LC/MS (ACN), and trifluoroacetic acid for HPLC (TFA) were obtained from Tokyo Chemical Industry Co., Ltd. Chloroform for HPLC was obtained from Kishida Chemical.

Preparation of standard solution To prepare standard solutions, each standard was dissolved in 50% MeOH (MeOH/water = 1/1, v/v), 50% MeOH–0.02 mol/L-HCl (for DL-glutamic acid, DL-histidine and DL-tryptophan), or 50% MeOH–0.05 mol/L-HCl (for DL-aspartic acid and DL-tyrosine). Standard solutions were diluted to obtain mixture solutions of each compound at 0.001, 0.005, 0.01, 0.05, 0.1, 0.5, 1, 5, 10, and 50 nmol/mL (the value means each enantiomer's concentration, not sum of enantiomers). A solution of DL-alanine-d_4 was prepared as described above (20 μmol/mL (both D-, and L-alanine-d_4: 10 μmol/mL) in MeOH/water = 1/1, v/v) and used as an internal standard. All data were corrected by peak area of D-alanine-d_4 to reduce analytic errors.

Sample pretreatment Sample extraction was essentially performed in accordance to a previously reported method (25). Commercially available cheeses aged 6, 18, and 26 months (Beemester, North Holland, the Netherlands) were prepared. Fifty milligrams of frozen cheese samples were powdered by a Multi-beads shocker (Yasui Kikai, Osaka, Japan) at 1000 rpm for 10 s and dissolved in 500 μL of MeOH. Fifty microliters of samples solution diluted 2-, 5-, or 50-fold with water were mixed with 350 μL of MeOH, 100 μL of water, and 20 μL of internal standard solution in a 1.5-mL tube, followed by vortex mixing and centrifugation at 10,000 rpm for 10 min at 4°C. Then, 360 μL of supernatant was transferred to a new 1.5-mL tube and mixed with 180 μL of water and 360 μL of chloroform. After vortexing and centrifugation in the same conditions described above, 50 μL of supernatant was diluted with 200 μL of ACN-EtOH mixed solution. Approximately 100 μL of diluted sample was transferred to a vial and subjected to LC/MS analysis. Standard solutions were also pretreated using the same method as the cheese samples to obtain calibration curves for quantification.

LC-MS analysis LC-MS/MS analysis was performed using the Nexera HPLC System (Shimadzu Corporation, Kyoto, Japan) connected to an LCMS-8060 (Shimadzu) with dual ion source of electrospray ionization and atmospheric pressure chemical ionization in MRM mode. The ion source was operated in positive mode and the interface parameters were optimized under the following conditions: nebulizer gas: 3 L/min; heating gas: 15 L/min; drying gas: 5 L/min; interface temperature: 200°C; desolvation line temperature: 250°C; heat block temperature: 300°C and interface voltage: 4 kV. To optimize the MRM transition, a 100 nmol/mL standard solution was injected into the triple quadrupole mass spectrometry without any columns. The standard solution contains a single compound; otherwise, a wrong transition can be employed when MS/MS recognize some compounds which has similar molecular weight. Chromatographic separation was achieved with CROWNPAK CR-I (+)/CR-I (−) (3.0 mm i.d. × 150 mm, 5 μm) and CHIRALPAK ZWIX (−) (4.0 mm i.d. × 150 mm, 3 μm) (Daicel CPI, Osaka, Japan) as the analytical columns. The injection volume was 1 μL and the oven temperature was kept at 30°C. The mobile phase consisted of a mixture of ACN, EtOH, water, and TFA (80/15/5/0.5, v/v/v/v) for CR-I (+)/(−) column, and 25 mM FA+ 25 mM AF in MeOH and water (98/2, v/v) for ZWIX (−) column. The flow rate was set to 0.4 mL/min in isocratic conditions. Data acquisition and processing were performed using LabSolutions (Shimadzu).

Statistical analysis LC-MS data were integrated into Excel sheets from LabSolutions. Among them, peak area values (with internal standard correction) were applied to principal component analysis (PCA). PCA was performed using a commercial software, SIMCA-P+ version 12 (Umetrics, Umeå, Sweden). All data were standardized to autoscale (mean = 0, variance = 1) prior to calculation.

TABLE 1. Optimized MRM transitions and MS parameters.

	Precursor ion (*m/z*)	Product ion (*m/z*)	Q1 Pre Bias (V)	CE (eV)	Q3 Pre Bias (V)
Ethanolamine	62.20	44.15	−27	−12	−17
Glycine	76.20	29.90	−10	−11	−28
Alanine	90.10	44.10	−10	−14	−17
Sarcosine	90.20	44.20	−30	−13	−17
β-Alanine	90.20	72.15	−30	−11	−30
d4-Alanine	94.15	48.20	−13	−19	−15
α-Aminobutyric acid	104.05	58.00	−28	−12	−23
N,*N*-Dimethylglycine	104.05	58.10	−30	−15	−26
γ-Aminobutyric acid	104.05	87.10	−29	−11	−16
Serine	106.10	42.10	−11	−20	−16
Hypotaurine	110.15	92.10	−10	−12	−16
Cytosine	112.05	95.10	−10	−22	−21
Histamine	112.10	95.10	−29	−16	−18
Uracil	113.20	70.00	−11	−18	−29
Creatinine	114.05	70.00	−28	−18	−19
Proline	116.10	70.10	−11	−16	−12
Betaine	118.10	58.10	−28	−28	−24
Valine	118.10	72.05	−11	−12	−13
Norvaline	118.10	72.15	−11	−11	−29
2,4-Diaminobutyric acid	119.10	56.10	−11	−22	−23
Threonine	120.10	74.00	−11	−12	−13
Homoserine	120.10	74.00	−10	−13	−30
Cysteine	122.05	59.00	−10	−24	−22
Nicotinamide	123.05	80.15	−30	−22	−30
Nicotinic acid	124.05	80.15	−11	−22	−14
Thymine	127.20	110.10	−11	−17	−26
Pipecolic acid	130.10	84.10	−12	−18	−17
N-Acetylalanine	132.05	90.10	−30	−10	−16
Leucine	132.10	86.15	−11	−12	−18
Isoleucine	132.10	86.15	−13	−12	−18
Creatine	132.25	90.10	−14	−13	−16
Ornithine	133.10	70.10	−12	−16	−28
Asparagine	133.10	74.05	−10	−17	−14
Glycylglycine	133.20	76.15	−13	−11	−30
Aspartic acid	134.20	74.10	−16	−15	−14
Adenine	136.05	119.10	−30	−23	−16
Anthranilic acid	138.05	120.10	−30	−14	−24
Tyramine	138.20	121.20	−14	−15	−25
Glutamine	147.10	84.10	−18	−18	−16
Lysine	147.10	84.10	−17	−18	−21
Glutamic acid	148.10	84.10	−10	−17	−18
Methionine	150.10	56.10	−10	−17	−18
Guanine	152.05	135.15	−14	−21	−23
Dopamine	154.10	91.15	−14	−24	−19
Histidine	156.10	110.10	−12	−15	−11
Tryptamine	161.25	144.10	−16	−12	−29
2-Aminoadipic acid	162.10	98.15	−15	−17	−10
Ethionine	164.10	75.05	−13	−22	−30
Phenylalanine	166.10	120.10	−10	−14	−12
Arginine	175.10	70.10	−17	−24	−12
2-Aminopimelic acid	176.10	112.20	−13	−15	−11
Citrulline	176.10	70.20	−17	−23	−27
Carbamoyl aspartic acid	177.15	74.10	−16	−22	−29
Serotonin	177.25	160.10	−18	−10	−29
Homophenylalanine	180.20	91.10	−19	−26	−17
Tyrosine	182.10	136.00	−10	−14	−23
2-Aminosuberic acid	190.20	126.15	−19	−15	−24
Dopa	198.20	107.05	−10	−26	−17
Tryptophan	205.10	188.15	−11	−10	−12
Kynurenine	209.20	192.10	−10	−8	−20
N-Acetylserotonin	219.05	160.05	−20	−15	−30
5-Hydroxytryptophan	221.15	204.15	−22	−11	−21
Cystathionine	223.15	88.05	−22	−27	−16
Melatonin	233.20	174.10	−24	−18	−19
Cystine	240.95	74.15	−21	−29	−28
Thymidine	243.20	127.10	−12	−11	−23
Cytidine	244.20	112.10	−12	−12	−11
Uridine	245.00	113.00	−23	−11	−21
Adenosine	267.95	136.10	−22	−16	−23
Inosine	268.95	137.00	−20	−20	−20
Guanosine	283.95	151.95	−27	−18	−26

CE, collision energy.

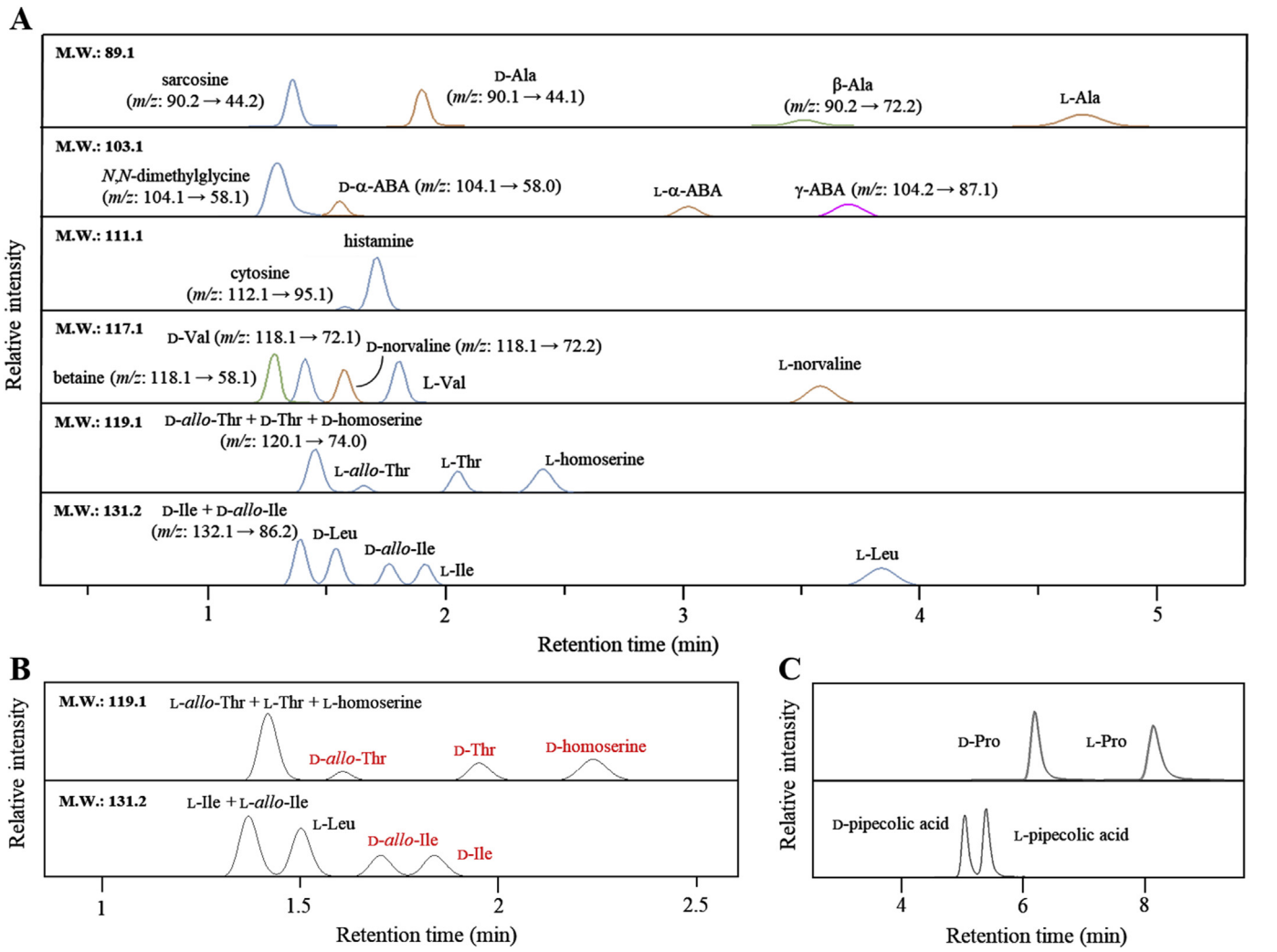

FIG. 1. The chromatograms obtained by CROWNPAK CR-I (+), CR-I (−) and CHIRALPAK ZWIX (−). (A) Partial chromatograms of targeted compounds with the same molecular weight obtained by LC-MS/MS analysis using CROWNPAK CR-I (+). These chromatograms were obtained from a 1 nmol/mL mix standard solution (Ala, alanine; ABA, aminobutyric acid; Val, valine; Thr, threonine; Ile, isoleucine; and Leu, leucine). The same color peaks were detected in the same MRM transition. Most compounds showed baseline separation while some compounds including D-*allo*-Thr, D-Thr, and D-homoserine or D-Ile and D-*allo*-Ile co-eluted. (B) Extracted ion chromatograms using CROWNPAK CR-I (−). The chromatogram for the MRM transition of *m/z* 120.1 to 74.0 (molecular weight: 119.1) and 132.1 to 86.2 (molecular weight: 131.2). The CR-I (−) column reversed the elution order for each compound from the CR-I (+) column. (C) A part of chromatogram of secondary amines by using CHIRALPAK ZWIX (−). The ZWIX column, with zwitterionic molecules that incorporated both anion- and cation-exchange functional groups, enabled the separation of secondary amines including proline (Pro).

RESULTS AND DISCUSSION

Optimization of MS parameters and separation of targeted compounds To construct an LC-MS/MS system for the highly sensitive detection of wide-targeted chiral metabolites, we optimized several MS parameters. We first optimized the MRM transitions of targeted metabolites. MS/MS detected $[M + H]^+$ ions as the precursor ion of all targeted compounds. The product ions were highly dependent on the collision energy (CE) and the MS/MS electrical parameters including CE, Q1 Pre Bias, and Q3 Pre Bias were optimized to obtain the highest sensitivity (Table 1). The electrospray probe position was also adjusted because the position could be closely related to the desolvation and ionization efficiency in electrospray ionization (26). The position parameters were decided at 1 mm intervals (min: +1 mm (P1), max: +6 mm (P6)) from the default position using 36 mix standards which showed relatively lower sensitivity (Fig. S1). The sensitivity increased dramatically by increasing the distance from the default probe position, but sensitivity decreased towards the maximum distance. This might be a result of reducing the number of ions into the inlet of the mass spectrometer. Most compounds indicated the highest sensitivities at +4 mm (P4) position as shown in Fig. S1.

Next, we confirmed the separation of targeted compounds using the optimized conditions. Chromatographic conditions were determined according to our previous report using LC-TOFMS and LC-MS/MS methods (23–25). In these methods, we employed chiral columns (CROWNPAK CR-I (+) and CROWNPAK CR-I (−)) for enantioseparation of targeted amino acids and amines. These columns contain binaphthyl skeleton-based crown ether as a chiral selector for enantioseparation. The crown ether strongly interacts with amino groups that are protonated by the highly acidic mobile phase. Then, the binaphthyl part causes stereospecific retention due to the structural difference of enantiomers. We applied this estimated separation principle in this study and targeted compounds were successfully separated, even the compounds of the same molecular weight, in MRM mode (Fig. 1A). Most compounds demonstrated high-resolution separation and symmetric peak shape. However, as Fig. 1A shows, some compounds coeluted at the same retention time (e.g., D-*allo*-threonine, D-threonine, and

TABLE 2. Evaluation results of the LC-MS/MS method.

	Column	RT (min)	Range (nmol/mL)	*r* value	RSD (%)	LOD (nmol/mL)
N,*N*-Dimethylglycine	CR-I (+)	1.305	0.001–1	0.9940	1.5	0.001
Betaine	CR-I (+)	1.308	0.001–10	0.9933	3.0	0.001
Sarcosine	CR-I (+)	1.360	0.05–10	0.9983	3.6	0.05
Creatine	CR-I (+)	1.367	0.01–10	0.9985	1.8	0.01
D-Arginine	CR-I (+)	1.369	0.001–10	0.9981	0.8	0.001
D-Histidine	CR-I (+)	1.375	0.01–10	0.9980	4.0	0.01
D-Valine	CR-I (+)	1.414	0.001–10	0.9987	4.6	0.001
Creatinine	CR-I (+)	1.460	0.005–10	0.9981	2.8	0.005
D-Glutamine	CR-I (+)	1.503	0.005–10	0.9978	5.6	0.005
D-Asparagine	CR-I (+)	1.528	0.05–10	0.9978	9.3	0.05
L-Histidine	CR-I (+)	1.529	0.01–50	0.9971	0.4	0.01
Nicotinamide	CR-I (+)	1.537	0.005–10	0.9964	10.4	0.005
D-Phenylalanine	CR-I (+)	1.547	0.05–10	0.9989	2.9	0.05
D-Leucine	CR-I (+)	1.550	0.005–10	0.9987	7.3	0.005
D-Tyrosine	CR-I (+)	1.553	0.005–10	0.9947	10.3	0.005
D-Tryptophan	CR-I (+)	1.553	0.001–10	0.9975	5.2	0.001
Nicotinic acid	CR-I (+)	1.554	0.001–10	0.9981	7.0	0.001
D-5-Hydroxytryptophan	CR-I (+)	1.554	0.001–10	0.9978	6.2	0.001
Cytidine	CR-I (+)	1.568	0.001–10	0.9989	2.9	0.001
D-Dopa	CR-I (+)	1.574	0.001–10	0.9970	5.2	0.001
Cytosine	CR-I (+)	1.574	0.005–50	0.9986	5.6	0.005
D-α-Aminobutyric acid	CR-I (+)	1.576	0.01–10	0.9982	2.6	0.01
D-Norvaline	CR-I (+)	1.578	0.005–10	0.9965	5.6	0.005
D-2-Aminoadipic acid	CR-I (+)	1.614	0.001–10	0.9977	2.1	0.001
Adenosine	CR-I (+)	1.617	0.001–10	0.9960	2.6	0.001
D-2-Aminopimelic acid	CR-I (+)	1.619	0.005–10	0.9983	2.0	0.005
Adenine	CR-I (+)	1.626	0.001–10	0.9972	3.2	0.001
D-2-Aminosuberic acid	CR-I (+)	1.631	0.001–10	0.9981	1.5	0.001
D-Citrulline	CR-I (+)	1.631	0.01–50	0.9957	2.2	0.01
D-Cysteine	CR-I (+)	1.662	0.005–50	0.9984	3.3	0.005
Cystathionine-1	CR-I (+)	1.666	0.001–50	0.9938	0.4	0.001
D-Serine	CR-I (+)	1.699	0.05–10	0.9977	4.1	0.05
L-*allo*-Threonine	CR-I (+)	1.670	0.05–50	0.9947	6.2	0.05
D-Glutamic acid	CR-I (+)	1.722	0.005–50	0.9944	4.4	0.005
Histamine	CR-I (+)	1.722	0.005–50	0.9984	0.8	0.005
Guanosine	CR-I (+)	1.724	0.001–10	0.9986	2.5	0.001
Guanine	CR-I (+)	1.728	0.001–50	0.9987	2.4	0.001
D-Methionine	CR-I (+)	1.736	0.001–50	0.9957	5.7	0.001
D-Aspartic acid	CR-I (+)	1.740	0.01–10	0.9973	3.7	0.01
D-Ethionine	CR-I (+)	1.744	0.001–10	0.9978	3.2	0.001
D-2,4-Diaminobutyric acid	CR-I (+)	1.777	0.005–50	0.9973	4.7	0.005
L-*allo*-Isoleucine	CR-I (+)	1.777	0.01–50	0.9953	1.9	0.01
D-Homophenylalanine	CR-I (+)	1.811	0.001–10	0.9980	0.8	0.001
L-Valine	CR-I (+)	1.817	0.001–50	0.9956	4.2	0.001
L-Asparagine	CR-I (+)	1.821	0.05–50	0.9940	3.3	0.05
D-Kynurenine	CR-I (+)	1.860	0.005–50	0.9951	2.4	0.005
DD-Cystine	CR-I (+)	1.865	0.005–50	0.9964	2.4	0.005
D-Alanine	CR-I (+)	1.917	0.05–50	0.9969	7.2	0.05
L-Isoleucine	CR-I (+)	1.934	0.005–50	0.9981	6.7	0.005
L-Arginine	CR-I (+)	1.985	0.001–50	0.9962	2.9	0.001
L-Threonine	CR-I (+)	2.050	0.01–50	0.9982	5.3	0.01
L-2,4-Diaminobutyric acid	CR-I (+)	2.120	0.05–50	0.9830	2.3	0.05
Anthranilic acid	CR-I (+)	2.137	0.05–50	0.9970	14.6	0.05
D-Ornithine	CR-I (+)	2.157	0.05–10	0.9942	2.2	0.05
Thymine	CR-I (+)	2.172	0.05–50	0.9993	13.0	0.05
Thymidine	CR-I (+)	2.177	0.001–50	0.9985	5.6	0.001
Melatonin	CR-I (+)	2.200	0.001–5	0.9968	1.6	0.001
Uracil	CR-I (+)	2.223	0.1–50	0.9963	17.7	0.1
Uridine	CR-I (+)	2.227	0.005–50	0.9961	5.4	0.005
N-Acetylserotonin	CR-I (+)	2.285	0.005–10	0.9988	1.8	0.005
L-Serine	CR-I (+)	2.336	0.1–10	0.9962	6.4	0.1
Inosine	CR-I (+)	2.377	0.001–10	0.9986	1.7	0.001
L-Homoserine	CR-I (+)	2.408	0.05–50	0.9993	2.3	0.05
L-5-Hydroxytryptophan	CR-I (+)	2.535	0.001–50	0.9993	0.7	0.001
L-Tryptophan	CR-I (+)	2.561	0.005–50	0.9998	1.5	0.005
Cystathionine-2	CR-I (+)	2.579	0.005–50	0.9976	1.7	0.005
L-Tyrosine	CR-I (+)	2.602	0.01–50	0.9994	1.6	0.01
L-Aspartic acid	CR-I (+)	2.647	0.05–50	0.9995	7.0	0.05
L-Phenylalanine	CR-I (+)	2.680	0.05–50	0.9999	1.3	0.05
L-Dopa	CR-I (+)	2.717	0.001–50	0.9992	2.7	0.001
L-Cysteine	CR-I (+)	2.940	0.005–50	0.9996	2.9	0.005
L-α-Aminobutyric acid	CR-I (+)	2.990	0.01–50	0.9998	0.8	0.01
Tyramine	CR-I (+)	3.201	0.005–50	0.9994	1.4	0.005
Ethanolamine	CR-I (+)	3.244	0.05–50	0.9997	11.1	0.05
Dopamine	CR-I (+)	3.331	0.005–50	0.9997	2.3	0.005
Serotonin	CR-I (+)	3.347	0.001–50	0.9999	1.0	0.001
Glycylglycine	CR-I (+)	3.380	0.005–50	0.9988	0.8	0.005
L-Citrulline	CR-I (+)	3.411	0.005–50	0.9998	2.2	0.005
Tryptamine	CR-I (+)	3.431	0.001–50	0.9983	1.1	0.001
β-Alanine	CR-I (+)	3.519	0.1–50	0.9999	11.3	0.1
L-Norvaline	CR-I (+)	3.592	0.01–50	0.9998	2.4	0.01
L-Kynurenine	CR-I (+)	3.691	0.005–50	0.9999	1.8	0.005
γ-Aminobutyric acid	CR-I (+)	3.709	0.005–50	0.9998	2.1	0.005
Glycine	CR-I (+)	3.717	0.05–50	0.9994	3.8	0.05
L-2-Aminopimelic acid	CR-I (+)	3.739	0.005–50	0.9995	2.4	0.005
Hypotaurine	CR-I (+)	3.795	0.05–50	0.9995	1.9	0.05
L-Leucine	CR-I (+)	3.850	0.005–50	0.9999	1.5	0.005
L-2-Aminosuberic acid	CR-I (+)	3.858	0.005–50	0.9998	2.5	0.005
meso-Cystine	CR-I (+)	3.960	0.005–50	0.9987	2.0	0.005
L-2-Aminoadipic acid	CR-I (+)	4.017	0.005–50	0.9999	2.8	0.005
L-Ornithine	CR-I (+)	4.086	0.05–50	0.9986	3.2	0.05
Cystathionine-3	CR-I (+)	4.477	0.005–50	0.9999	0.9	0.005
L-Alanine	CR-I (+)	4.684	0.05–50	0.9997	4.4	0.05
L-Glutamic acid	CR-I (+)	5.123	0.005–50	0.9997	1.5	0.005
L-Ethionine	CR-I (+)	5.196	0.005–50	0.9998	0.8	0.005
L-Methionine	CR-I (+)	5.257	0.005–50	0.9996	1.0	0.005
L-Homophenylalanine	CR-I (+)	5.970	0.001–50	0.9998	1.0	0.001
L-Lysine	CR-I (+)	7.478	0.005–50	0.9999	0.5	0.005
Cystathionine-4	CR-I (+)	10.606	0.005–50	0.9997	1.9	0.005
LL-Cystine	CR-I (+)	15.762	0.005–50	0.9999	1.8	0.005
L-Glutamine	CR-I (−)	1.448	0.001–10	0.9977	7.5	0.001
D-*allo*-Threonine	CR-I (−)	1.613	0.001–10	0.9998	7.8	0.001
D-*allo*-Isoleucine	CR-I (−)	1.702	0.001–10	1.0000	4.5	0.001
D-Isoleucine	CR-I (−)	1.839	0.001–10	1.0000	4.9	0.001
D-Threonine	CR-I (−)	1.959	0.001–10	0.9999	5.0	0.001
D-Homoserine	CR-I (−)	2.244	0.001–10	1.0000	6.7	0.001
D-Lysine	CR-I (−)	6.423	0.001–10	0.9997	14.0	0.001
L-*N*-Acetylalanine	ZWIX (−)	3.992	0.005–10	0.9999	0.3	0.005
D-Pipecolic acid	ZWIX (−)	5.249	0.005–50	0.9987	1.2	0.005
D/L-Carbamoyl aspartic acid	ZWIX (−)	5.339	0.01–50	0.9986	0.2	0.01
D/L-Carbamoyl aspartic acid	ZWIX (−)	5.674	0.05–50	0.9963	0.1	0.05
L-Pipecolic acid	ZWIX (−)	5.726	0.005–50	0.9999	16.8	0.005
D-*N*-Acetylalanine	ZWIX (−)	5.977	0.005–50	0.9968	4.4	0.005
D-Proline	ZWIX (−)	6.171	0.005–10	0.9997	3.0	0.005
L-Proline	ZWIX (-)	8.194	0.005–10	0.9990	10.2	0.005

(*continued on next page*)

TABLE 2 (*continued*)

RT, retention time; RSD, relative standard deviation; LOD, limit of detection. Cystathionine-1, -2, -3, -4, and D/L-carbamoyl aspartic acid are one of forms among conceivable enantiomers (no identification due to the lack of commercially available standard of single enantiomer).

D-homoserine). To solve this problem, we employed another chiral crown ether column. CROWNPAK CR-I (+) was selected as an enantioseparation column that retained D-amino acids more weakly and eluted them before L-amino acids. Furthermore, CROWNPAK CR-I (−), which contains the axial chiral structure of selector in stationary phase of CR-(+) ((*S*)-18-crown-6-ether for CR-I (+), (*R*)-18-crown-6-ether for CR-I (−)), can reverse the elution order of enantiomers. The coeluted compounds were successfully separated using this column (Fig. 1B). Moreover, we investigated the enantioseparation of secondary amines that could not be separated using CROWNPAK CR-I (+) and CR-I (−) due to the poor affinity between the crown ether and the amino group of secondary amines. A column screening was performed and some secondary amines, including proline, were enantiomerically separated using CHIRALPAK ZWIX (−) (Fig. 1C). This column contains cinchona alkaloid-derived zwitterionic chiral stationary phases. It is assumed that the analyte cation interacts with the anionic site of the chiral selector and the analyte anion interacts with the cationic site of the chiral selector through a strong coulombic attraction, which led to synergetic double ion-pairing between the chiral selector and the analyte (27). For the intra-molecular counterion effect of the chiral selectors in ZXIX (−), the mobile phase must contain acidic and

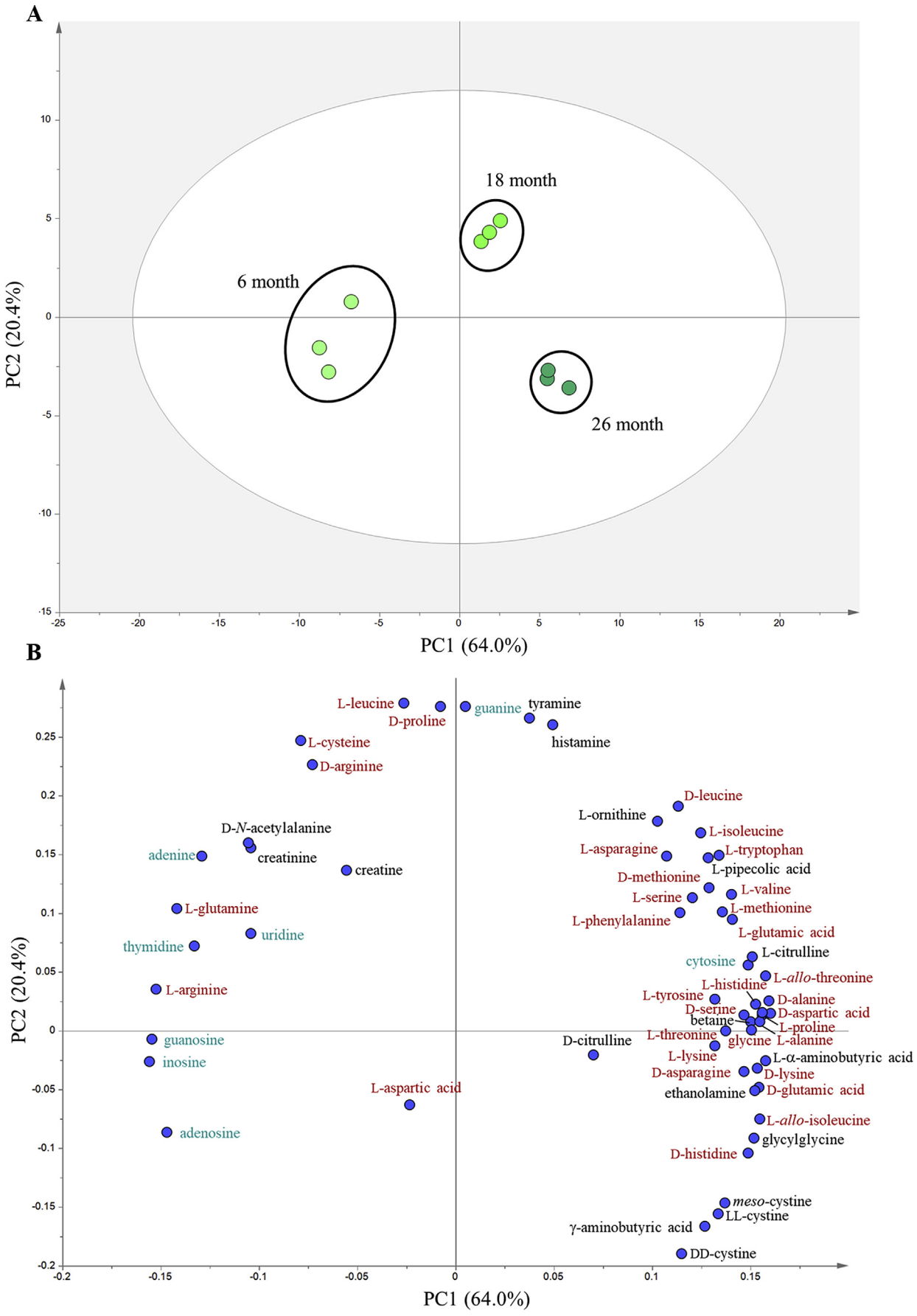

FIG. 2. The result of PCA of the component profile data. (A) Score plot. (B) Loading plot. Red compounds are proteinogenic amino acids and their enantiomers, and blue compounds are nucleic acid metabolites.

basic additives. In most cases, diethylamine or triethylamine are employed as the basic additives (28,29), but using these materials at high concentrations may contaminate the MS. Therefore, we used a combination of formic acid and ammonium formate instead of diethylamine or trimethylamine as other research has recently reported (30). The combination of these columns enabled the comprehensive analysis of 115 compounds including both chiral primary and secondary amines. The chromatograms of other compounds are shown in Figs. S2–S4.

Moreover, we also examined the MS ion source gas parameters such as nebulizer gas (NG), heating gas (HG), and drying gas (DG). Gas flow is also one of the most important parameters for the desolvation of analyte ions. The NG flow rate was investigated at 1, 2, and 3 L/min. The HG and DG flow rates were investigated with the following combinations: HG, 5 L/min; DG, 15 L/min; HG, 10 L/min; DG, 10 L/min; and HG, 15 L/min; DG, 5 L/min (Fig. S5). The maximum sensitivity was obtained at 3 L/min (NG), 15 L/min (HG), and 5 L/min (DG). Finally, we optimized MS heat parameters such as interface temperature (IF), heat block temperature (HB), and desolvation line temperature (DL). Each heat parameter was investigated at 150°C, 200°C, and 250°C (IF); 250°C, 300°C, and 350°C (HB); and 200°C, 250°C, and 300°C (DL) (Fig. S6). Ion source heating may aid desolvation and ionization, but interestingly, high IF decreased the relative sensitivity, and high HD and DL also did not improve sensitivity. The highest sensitivity was observed at 200°C (IF), 300°C (HB), and 250°C (DL). Consequently, the fine-tuning of physical, electric, gas, and heat parameters achieved over 5–10 times more sensitivity than our previous method.

Evaluation of the method We evaluated the developed LC-MS/MS analytical system for linearity of the dilution curve, practicality of the linear range, limits of detection (LOD), and repeatability (Table 2). The linearity of the dilution curve and the usable linear range were assessed with a standard mixture at concentrations of 0.001, 0.005, 0.01, 0.05, 0.1, 0.5, 1, 5, 10, and 50 nmol/mL for each compound. Linearity was evaluated by the correlation coefficient, the r value. Eleven compounds (cystathionine-1, guanine, D-methionine, L-valine, L-arginine, thymidine, L-5-hydroxytryptophan, L-dopa, serotonin, tryptamine, and L-homophenylalanine) showed linearity within a maximum range of 0.001–50 nmol/mL, and a minimum range of 0.1–10 nmol/mL for L-serine. The linearity of all dilution curves in wide range was confirmed with r values >0.99 (the mean value: 0.9980), indicating good correlation of the data and that the system was capable of quantifying concentrations of targeted compounds. The LOD was determined as the concentration that would give a signal-to-noise ratio of 3:1. The LOD ranged from 0.005 nmol/mL to 0.1 nmol/mL. The repeatability was evaluated from a relative standard deviation (RSD) of the peak area obtained from three successive analyses of a standard mixture. Our result showed that targeted compounds exhibited a mean RSD value of 3.9% at 0.5 nmol/mL, and all RSD values were $\leq$20%, indicating that the system maintained high repeatability.

There are several reports of method development for trace chiral metabolites focusing on D-amino acid analysis using LC-MS/MS (31–33). In these reports, the methods were sensitive enough to detect trace D-amino acids in biological samples, although the derivatization of analytes was essential. Conversely, our system provides a simple analytical method that does not require derivatization and has a great potential for wide-range detection of trace chiral metabolites in real samples.

Application to food samples To verify the applicability of our analysis system using LC-MS/MS, we applied this method to food samples. We prepared commercial natural cheeses with different ripening periods (6, 18, and 26 months). The taste and quality of cheese highly depends on metabolites produced during the manufacturing process, and the ripening process especially affects the amount and variety of metabolites (34,35). Further, some reports indicate that natural cheese may contain several D-amino acids originating from microorganisms (36,37). However, there are no reports on the simultaneous analysis of metabolites including D-, and L-amino acids. Thus, we verified whether our method enabled comprehensive profiling of both chiral and achiral compounds in real samples. First, three types of cheeses were pretreated to remove impurities and diluted for LC-MS/MS analysis. Unlike standard solutions, real samples have impurities that may affect the quality of quantitative analysis due to the matrix effect and loss from pretreatment procedures. We pretreated samples in accordance with the optimized method for D-amino acid analysis (25). Matrix factor was calculated from the ratio of area values obtained from the comparison of beforehand extracted cheese samples spiked with standard solution (2.5 nmol/mL) and a blank (dilution solution pretreated as well as cheese samples) spiked with the same standard solution. Peak area values were corrected to the internal standard (D-alanine-d_4) and the effect of endogenous targeted metabolites in cheeses were also considered for the calculation. The calculated average values were 90%, 95%, and 100% in 6-, 18-, and 26-month cheeses, respectively. Metabolites in cheeses were quantified using the calibration curve with peak area values of each standard. The standard solution for the calibration curve was also pretreated in the same procedure as the cheese samples to correct for extraction errors. A CROWNPAK CR-I (+) column was mainly used for the simultaneous separation of targeted metabolites while the peak identification of D-lysine, L-glutamine, D-threonine, D-*allo*-threonine and D-homoserine, D-isoleucine, D-*allo*-isoleucine were conducted using CR-I (−). Secondary amines such as D-, and L-proline were analyzed using ZWIX (−). Consequently, we detected 59 metabolites and successfully quantified their concentrations in each cheese (N = 3), while some metabolites' sensitivities were too low to quantify (Table S1). The detected metabolites included proteinogenic and nonproteinogenic D- and L-amino acid, amines, nucleic acid bases, and nucleosides. The profiling revealed that ripening period had a significant impact on the production of each metabolite, as previous studies have already shown (38,39). Interestingly, while some metabolites increased during ripening, other metabolites decreased. This phenomenon may contribute to the complexity of taste due to biochemical changes in cheese. The MRM chromatograms obtained from sample analysis are demonstrated in Fig. S7.

To assess the data structures clearly, we performed PCA using the peak area ratio of detected metabolites in cheeses (Fig. 2A and B). The first and second principal components (PCs) represented 64.0% and 20.4% of the total variance of the samples, respectively. The score plot indicated that samples scored according to the ripening period in PC1. In the loading plot, 26 proteinogenic D- and L-amino acids were positively correlated to PC1. This result is reasonable because levels of amino acids may increase due to various biochemical events, such as proteolysis (40,41). However, most nucleic acid metabolites, including nucleosides, contributed negatively to PC1. This suggests that microbes utilize carbohydrates derived from nucleosides, such as ribose, as an energy source for growth (42). Intriguingly, some D- and L-amino acids were located separately in different sides. For example, while D-leucine and L-proline were in the positive side of PC1, L-leucine and D-proline were in the positive side of PC2. According to the PCA results, some chiral amino acids exhibited characteristic profiles depending on the different cheese ripening period. When comparing the data of 6- and 18-month cheeses, all detected D-amino acids increased, whereas some L-amino acids decreased. As the ripening proceeded, most L-amino acids decreased further. Also, in order to discuss the time-course changes derived from ripening, we calculated

enantiomeric excess (e.e.) of amino acids (Table S2). The e.e. was obtained from quantified data of each D, and L-amino acid using the following formula:

$$\text{e.e. } (\%) = (L - D)/(L + D) \times 100 \quad (1)$$

where L and D is the mean value of quantified L- and D-amino acid, respectively. Most of the e.e. of amino acids showed 100% because L-amino acid predominantly exists in cheeses compared to each D-form. Since alanine was quantified in relatively similar amounts, the e.e. demonstrated around 20–30%. For aspartic acid, a drastic increase was observed as ripening proceeded, which indicates some metabolic reaction (e.g., isomerization) may be fluently occurred through the ripening process. Arginine remarkably showed the largest changes from 4% (6 months) to −55% (26 months). This trend may be explained by the major consumption of L-arginine due to its catabolism to counteract the acid stress and an alternative source of energy in natural cheese ripening (43). The fine profiling considering the chirality of metabolites has the possibility to reveal new insights into sensory characteristics, since the taste of D- and L-amino acids differs. These results showed that our novel method could be a powerful tool for higher-resolution metabolic profiling of foods.

In conclusion, we developed a simultaneous analytical system for wide-targeted chiral metabolomics using LC-MS/MS in MRM mode, and successfully applied this method toward analysis of a food sample. In particular, this method highlights the highly sensitive detection of trace amounts of targeted metabolites without the need for derivatization. Moreover, we demonstrated the usefulness of our system by simultaneously analyzing both chiral and non-chiral metabolites in real samples with a wide coverage and dynamic range. According to the results of the profiling, some D- and L-amino acids exhibited different behaviors in the PCA plot, which could never be observed by conventional methods that do not consider separation of enantiomers. We anticipate that this new method will enable comprehensive profiling to provide novel insights into the discovery of molecular markers utilized in various fields, especially for food analysis.

Supplementary data to this article can be found online at https://doi.org/10.1016/j.jbiosc.2018.10.003.

ACKNOWLEDGMENTS

This study was partially supported by AMED-CREST under Grant Number JP18gm071000nd Grand-in-Aid for Challenging Research under Grant Number 17K19235. The study represents a portion of the dissertation submitted by Yosuke Nakano to Osaka University in partial fulfillment of the requirement for his Ph.D.

References

1. **Yoon, T. P. and Jacobsen, E. N.:** Privileged chiral catalysts, Science, **299**, 1691–1693 (2003).
2. **Liu, W., Gan, J., Schlenk, D., and Jury, W. A.:** Enantioselectivity in environmental safety of current chiral insecticides, Proc. Natl. Acad. Sci. USA, **102**, 701–706 (2005).
3. **Kasprzyk-Hordern, B.:** Pharmacologically active compounds in the environment and their chirality, Chem. Soc. Rev., **39**, 4466 (2010).
4. **Cava, F., Lam, H., de Pedro, M. A., and Waldor, M. K.:** Emerging knowledge of regulatory roles of D-amino acids in bacteria, Cell. Mol. Life Sci., **68**, 817–831 (2011).
5. **Ohide, H., Miyoshi, Y., Maruyama, R., Hamase, K., and Konno, R.:** D-Amino acid metabolism in mammals: biosynthesis, degradation and analytical aspects of the metabolic study, J. Chromatogr. B Analyt. Technol. Biomed. Life Sci., **879**, 3162–3168 (2011).
6. **Hashimoto, A., Nishikawa, T., Hayashi, T., Fujii, N., Harada, K., Oka, T., and Takahashi, K.:** The presence of free D-serine in rat brain, FEBS Lett., **296**, 33–36 (1992).
7. **Nishikawa, T.:** Analysis of free D-serine in mammals and its biological relevance, J. Chromatogr. B Analyt. Technol. Biomed. Life Sci., **879**, 3169–3183 (2011).
8. **Chumakov, I., Blumenfeld, M., Guerassimenko, O., Cavarec, L., Palicio, M., Abderrahim, H., Bougueleret, L., Barry, C., Tanaka, H., and La Rosa, P.:** Genetic and physiological data implicating the new human gene G72 and the gene for D-amino acid oxidase in schizophrenia, Proc. Natl. Acad. Sci. USA, **99**, 13675–13680 (2002).
9. **Ono, K., Shishido, Y., Park, H. K., Kawazoe, T., Iwana, S., Chung, S. P., Abou El-Magd, R. M., Yorita, K., Okano, M., and Watanabe, T.:** Potential pathophysiological role of D-amino acid oxidase in schizophrenia: immunohistochemical and in situ hybridization study of the expression in human and rat brain, J. Neural. Transm., **116**, 1335–1347 (2009).
10. **Cioffi, C. L.:** Modulation of NMDA receptor function as a treatment for schizophrenia, Bioorg. Med. Chem. Lett, **23**, 5034–5044 (2013).
11. **D'Aniello, S., Somorjai, I., Garcia-Fernàndez, J., Topo, E., and D'Aniello, A.:** D-Aspartic acid is a novel endogenous neurotransmitter, FASEB J., **25**, 1014–1027 (2011).
12. **Takigawa, Y., Homma, H., Lee, J. A., Fukushima, T., Santa, T., Iwatsubo, T., and Imai, K.:** D-Aspartate uptake into cultured rat pinealocytes and the concomitant effect on L-aspartate levels and melatonin secretion, Biochem. Biophys. Res. Commun., **248**, 641–647 (1998).
13. **Long, Z., Lee, J. A., Okamoto, T., Nimura, N., Imai, K., and Homma, H.:** d-Aspartate in a prolactin-secreting clonal strain of rat pituitary tumor cells (GH_3), Biochem. Biophys. Res. Commun., **276**, 1143–1147 (2000).
14. **Nagata, Y., Homma, H., Lee, J. A., and Imai, K.:** D-Aspartate stimulation of testosterone synthesis in rat Leydig cells, FEBS Lett., **444**, 160–164 (1999).
15. **Kimura, T., Hamase, K., Miyoshi, Y., Yamamoto, R., Yasuda, K., Mita, M., Rakugi, H., Hayashi, T., and Isaka, Y.:** Chiral amino acid metabolomics for novel biomarker screening in the prognosis of chronic kidney disease, Sci. Rep., **6**, 26137 (2016).
16. **Bhushan, R. and Parshad, V.:** Thin-layer chromatographic separation of enantiomeric dansylamino acids using a macrocyclic antibiotic as a chiral selector, J. Chromatogr. A, **736**, 235–238 (1996).
17. **Bhushan, R., Brückner, H., Kumar, V., and Gupta, D.:** Indirect TLC resolution of amino acid enantiomers after derivatization with Marfey's reagent and its chiral variants, J. Planar Chromatogr. Mod. TLC, **20**, 165–171 (2007).
18. **Bertrand, M., Chabin, A., Brack, A., and Westall, F.:** Separation of amino acid enantiomers VIA chiral derivatization and non-chiral gas chromatography, J. Chromatogr. A, **1180**, 131–137 (2008).
19. **Zahradnícková, H., Husek, P., and Simek, P.:** GC separation of amino acid enantiomers via derivatization with heptafluorobutyl chloroformate and Chirasil-L-Val column, J. Separ. Sci., **32**, 3919–3924 (2009).
20. **Bhushan, R. and Nagar, H.:** Indirect enantioseparation of proteinogenic amino acids using naproxen-based chiral derivatizing reagent and HPLC, Biomed. Chromatogr., **27**, 750–756 (2013).
21. **Cui, Y., Jiang, Z., Sun, J., Yu, J., Li, M., Li, M., Liu, M., and Guo, X.:** Enantiomeric purity determination of (L)-amino acids with pre-column derivatization and chiral stationary phase: development and validation of the method, Food Chem., **158**, 401–407 (2014).
22. **Hamase, K., Nakauchi, Y., Miyoshi, Y., Koga, R., Kusano, N., Onigahara, H., Naraoka, H., Mita, H., Kadota, Y., Nishio, Y., Mita, M., and Linder, W.:** Enantioselective determination of extraterrestrial amino acids using a two-dimensional chiral high-performance liquid chromatographic system, Chromatography, **35**, 103–110 (2014).
23. **Konya, Y., Bamba, T., and Fukusaki, E.:** Extra-facile chiral separation of amino acid enantiomers by LC-TOFMS analysis, J. Biosci. Bioeng., **121**, 349–353 (2016).
24. **Nakano, Y., Konya, Y., Taniguchi, M., and Fukusaki, E.:** Development of a liquid chromatography-tandem mass spectrometry method for quantitative analysis of trace d-amino acids, J. Biosci. Bioeng., **123**, 134–138 (2017).
25. **Konya, Y., Taniguchi, M., and Fukusaki, E.:** Novel high-throughput and widely-targeted liquid chromatography–time of flight mass spectrometry method for D-amino acids in foods, J. Biosci. Bioeng., **123**, 126–133 (2017).
26. **Janusson, E., Hesketh, A. V., Bamford, K. L., Hatlelid, K., Higgins, R., and McIndoe, J. S.:** Spatial effects on electrospray ionization response, Int. J. Mass Spectrom., **388**, 1–8 (2015).
27. **Tanwar, S. and Bhushan, R.:** Enantioresolution of amino acids: a decade's perspective, prospects and challenges, Chromatographia, **78**, 1113–1134 (2015).
28. **Pell, R., Sić, S., and Lindner, W.:** Mechanistic investigations of cinchona alkaloid-based zwitterionic chiral stationary phases, J. Chromatogr. A, **1269**, 287–296 (2012).
29. **Ilisz, I., Gecse, Z., Pataj, Z., Fülöp, F., Tóth, G., Lindner, W., and Péter, A.:** Direct high-performance liquid chromatographic enantioseparation of secondary amino acids on *Cinchona* alkaloid-based chiral zwitterionic stationary phases. Unusual temperature behavior, J. Chromatogr. A, **1363**, 169–177 (2014).
30. **Gerhardt, H., Sievers-Engler, A., Jahanshah, G., Pataj, Z., Ianni, F., Gross, H., Lindner, W., and Lämmerhofer, M.:** Methods for the comprehensive structural elucidation of constitution and stereochemistry of lipopeptides, J. Chromatogr. A, **1428**, 280–291 (2016).
31. **Visser, W. F., Verhoeven-Duif, N. M., Ophoff, R., Bakker, S., Klomp, L. W., Berger, R., and de Koning, T. J.:** A sensitive and simple ultra-high-

performance-liquid chromatography-tandem mass spectrometry based method for the quantification of D-amino acids in body fluids, J. Chromatogr. A, **1218**, 7130–7136 (2011).
32. **Reischl, R. J. and Lindner, W.:** Methoxyquinoline labeling–a new strategy for the enantioseparation of all chiral proteinogenic amino acids in 1-dimensional liquid chromatography using fluorescence and tandem mass spectrometric detection, J. Chromatogr. A, **1269**, 262–269 (2012).
33. **Karakawa, S., Shimbo, K., Yamada, N., Mizukoshi, T., Miyano, H., Mita, M., Lindner, W., and Hamase, K.:** Simultaneous analysis of D-alanine, D-aspartic acid, and D-serine using chiral high-performance liquid chromatography-tandem mass spectrometry and its application to the rat plasma and tissues, J. Pharm. Biomed. Anal., **115**, 123–129 (2015).
34. **Molimard, P. and Spinnler, H. E.:** Review: compounds involved in the flavor of surface mold-ripened cheeses: origins and properties, J. Dairy Sci., **79**, 169–184 (1996).
35. **Ochi, H., Naito, H., Iwatsuki, K., Bamba, T., and Fukusaki, E.:** Metabolomics-based component profiling of hard and semi-hard natural cheeses with gas chromatography/time-of-flight-mass spectrometry, and its application to sensory predictive modeling, J. Biosci. Bioeng., **113**, 751–758 (2012).
36. **Brückner, H., Jaek, P., Langer, M., and Godel, H.:** Liquid chromatographic determination of D-amino acids in cheese and cow milk. Implication of starter cultures, amino acid racemases, and rumen microorganisms on formation, and nutritional considerations, Amino Acids, **2**, 271–284 (1992).
37. **Csapó, J., Varga-Visi, É., Lóki, K., and Albert, C.:** The influence of manufacture on the free D-amino acid content of Cheddar cheese, Amino Acids, **32**, 39–43 (2007).
38. **Izco, J., Torre, P., and Barcina, Y.:** Ripening of Ossau-Iraty cheese: determination of free amino acids by RP-HPLC and of total free amino acids by the TNBS method, Food Contr., **11**, 7–11 (2000).
39. **McSweeney, P. L. H.:** Biochemistry of cheese ripening, Int. J. Dairy Technol., **57**, 127–144 (2004).
40. **Puchades, R., Lemieux, L., and Simard, R. E.:** Evolution of free amino acids during the ripening of cheddar cheese containing added lactobacilli strains, J. Food Sci., **54**, 885–888 (1989).
41. **Poveda, J. M., Cabezas, L., and McSweeney, P. L. H.:** Free amino acid content of Manchego cheese manufactured with different starter cultures and changes throughout ripening, Food Chem., **84**, 213–218 (2004).
42. **Smeianov, V. V., Wechter, P., Broadbent, J. R., Hughes, J. E., Rodríguez, B. T., Christensen, T. K., Ardö, Y., and Steele, J. L.:** Comparative high-density microarray analysis of gene expression during growth of *Lactobacillus helveticus* in milk versus rich culture medium, Appl. Environ. Microbiol., **73**, 2661–2672 (2007).
43. **D'Incecco, P., Gatti, M., Hogenboom, J. A., Bottari, B., Rosi, V., Neviani, E., and Pellegrino, L.:** Lysozyme affects the microbial catabolism of free arginine in raw-milk hard cheeses, Food Microbiol., **57**, 16–22 (2016).